Phosphatidylserine receptor is required for the engulfment of dead apoptotic cells and for normal embryonic development in zebrafish

Jiann-Ruey Hong[1,*], Gen-Hwa Lin[2], Cliff Ji-Fan Lin[2,3], Wan-ping Wang[2], Chien-Chung Lee[2], Tai-Lang Lin[2] and Jen-Leih Wu[2,*,†]

[1]Laboratory of Molecular Virology and Biotechnology, Institute of Biotechnology, National Cheng-Kung University, Tainan 701, Taiwan
[2]Laboratory of Marine Molecular Biology and Biotechnology, Institute of Zoology, Academia Sinica, Nankang, Taipei 115, Taiwan
[3]Graduate Institute of Life Sciences, National Defense Medical Center, Taipei 117, Taiwan
*These authors contributed equally
†Author for correspondence (e-mail: jlwu@gate.sinica.edu.tw)

Accepted 19 August 2004

Development 131, 5417-5427
Published by The Company of Biologists 2004
doi:10.1242/dev.01409

Summary

During development, the role of the phosphatidylserine receptor (PSR) in the removal of apoptotic cells that have died is poorly understood. We have investigated this role of PSR in developing zebrafish. Programmed cell death began during the shield stage, with dead cells being engulfed by a neighboring cell that showed a normal-looking nucleus and the nuclear condensation multi-micronuclei of an apoptotic cell. The zebrafish PSR engulfing receptor was cloned (*zfpsr*), and its nucleotide sequence was compared with corresponding sequences in *Drosophila melanogaster* (76% identity), human (74%), mouse (72%) and *Caenorhabditis elegans* (60%). The PSR receptor contained a jmjC domain (residues 143-206) that is a member of the cupin metalloenzyme superfamily, but in this case serves an as yet unknown function(s). *psr* knockdown by a PSR morpholino oligonucleotide led to accumulation of a large number of dead apoptotic cells in whole early embryo. These cells interfered with embryonic cell migration. In addition, normal development of the somite, brain, heart and notochord was sequentially disrupted up to 24 hours post-fertilization. Development could be rescued in defective embryos by injecting *psr* mRNA. These results are consistent with a PSR-dependent system in zebrafish embryos that engulfs apoptotic cells mediated by PSR-phagocytes during development, with the system assuming an important role in the normal development of tissues such as the brain, heart, notochord and somite.

Key words: Phosphatidylserine receptor, Apoptotic corpses, Zebrafish, Knockdown, Brain, Organogenesis

Introduction

Apoptotic cell death occurs by a mechanism that is conserved from nematodes to humans (Meier et al., 2000). In vivo, the typical fate for apoptotic cells is rapid engulfment and degradation by phagocytes (Savill, 1998). Amongst higher organisms, the removal of apoptotic cells by phagocytes suppresses inflammation, modulates the macrophage-directed deletion of host cells, and critically regulates the immune response of an individual (Savill and Fadok, 2000). For vertebrates, the phagocyte engages the dying cells through specific receptors that include the phospatidylserine receptor (PSR) (Fadok, 2000; Hong et al., 1998; Li, 2003), Fc receptors, complement receptors 3 and 4, the ABC1 transporter, and members of the scavenger-receptor family (Platt et al., 1998). For lower vertebrate systems such as the zebrafish, the cell corpses generated developmentally are quickly removed, although which specific type(s) of engulfment genes are involved still remains largely unknown.

Recent advances in the study of the nematode *Caenorhabditis elegans* (Chung et al., 2000; Wang et al., 2003) and *Drosophila melanogaster* (France et al., 1999a) illustrate the power of using genetically tractable systems to identify necessary phagocytic genes. Major efforts to understand crucial pathways that mediate programmed cell death have also led to the genetic and molecular characterization of a number of genes involved in the recognition and engulfment mechanisms of cells amongst invertebrates (Chung et al., 2000; Lauber et al., 2003; Arur et al., 2003; Ravichandran, 2003). For *C. elegans* it is important to recognize that phagocytosis is performed by cells that are non-specific phagocytes rather than by specialized phagocytes such as macrophages, as tends to be the case in *D. melanogaster* (Savill and Fadok, 2000).

Cell death that is morphologically and genetically distinct from apoptosis is strongly implicated in some human disease (Meier et al., 2000). Little is known regarding the molecular mechanisms by which the resulting (cell) corpses are eliminated, and the clearance of defective events for zebrafish. We sought to define the genetic requirements for a potentially distinct death paradigm associated with a loss-of-function of the cell-corpse receptor PSR in the zebrafish model system, to elucidate gene function related to organogenesis.

Morpholinos are chemically modified oligonucleotides with base-stacking abilities similar to those of natural genetic material (Summerton and Weller, 1997). Morpholinos have been shown to bind to and block translation of mRNA during cell genesis in zebrafish (Nasevicius and Ekker, 2000). Initially,

we cloned the *psr* gene from the 24 hours post-fertilization (hpf) cDNA library, and designed PSR morpholinos for the knockdown of PSR expression during the embryonic development of zebrafish. We found that a lot of apoptotic cells accumulated in the furrow or individual boundary of the whole somite, and interfered with the normal interior and posterior somitic formation at the early segmentation stage. At the post-segmentation and organogenesis developmental stages, the embryos were phenotypically defective in the brain, heart, somite and notochord. In addition, injection of *psr* mRNA with PSR morpholinos could compensate for the defective phenotype. These observations are consistent with an evolutionarily conserved pathway involving PSR that is responsible for the removal of cell corpses during cell migration, and for cell-cell interaction processes that are tightly linked to normal development during morphogenesis and organogenesis in zebrafish.

Materials and methods

Maintenance of fish line and embryo culture

Techniques for the care and breeding of zebrafish have been previously described in detail (Westerfield, 1993). Embryos were collected from natural matings and maintained in embryo medium (15 mM NaCl, 0.5 mM KCl, 1 mM $CaCl_2$, 1 mM $MgSO_4$, 0.15 mM, 0.05 mM Na_2HPO_4, 0.7 mM $NaHCO_3$) at 28.5°C. Embryos were staged according to standard morphological criteria (Kimmel et al., 1995).

Electron microscopy

Embryos at different developmental stages (30% epiboly, 50% epiboly, shield, 90% epiboly to tailbud) were collected with plastic droppers, placed in microtubes, washed twice with phosphate buffered saline (PBS), and then fixed with 2.5% glutaraldehyde in 0.1 M sodium cacodylate buffer (pH 7.2) for 2 hours. They were then washed with sodium cacodylate buffer, post-fixed in 1% aqueous osmium tetroxide for 2 hours, and washed with the same buffer. The embryos were dehydrated in a series of ethanol solutions and embedded in a Spurr's resin mixture using standard protocols. Semi-thin sections were cut, stained with Toluidine Blue, and examined by light microscopy (Nikon Eclipse E600, Nikon Corporation, Japan) to identify morphological patterns. Ultrathin sections, cut using a microtome, were stained with standard preparations of lead citrate and uranyl acetate, and observed using an electron microscope (Hitachi H-7000, Japan) (Hong et al., 1998).

PSR cloning

Two pairs of degenerate primers derived from human and *Drosophila* sequences (GenBank) (Fadok, 2000) were used to synthesize a 0.5 kb probe (by RT-PCR) to screen a 24-hour-old wild-type zebrafish (*Danio rerio*) embryo λ cDNA library (Stratagene). The degenerate primers used were as follows:

(1) PSR-5′P1, 5′-gAA(gA)TATCg(Cg)AACCAgAAgTTCAAgTg-(CT)gg(CT)gg(CT)gAgg-3′ (35mer);

(2) PSR 5′P2, 5-gt(Cg)AagATgAAgATgAA(gA)TACTAC(gA)T-(gC)gAgTACATg-3′ (36mer);

(3) PSR-3′P1, 5′CtggAAgAgTCgCTggAgCTgTC-3′; and

(4) PSR-3′P2, 5′-TtgAg(Cg)AC(AC)AC(Ag)TgCCAggAgCC(Tg)-CC(Tg)gg-3′.

The cDNA library was screened using low stringency conditions. The positive clones obtained were sequenced using a single-base reaction with the ABI Prism 377 DNA sequencer (Applied Biosystems, Foster City, CA, USA), according to the manufacturer's protocol. The following PSR homologs were acquired from GenBank: the human homolog KIAA 0585 (Nagase, 1998) (Accession number BAA25511); the mouse homolog AAH 06067 (Accession number AAG27719); the *D. melanogaster* homolog CG5383 (Accession number AF401485); the zebrafish homolog (Accession number AF401485. The *C. elegans* homolog was acquired from the cosmid F29B9.4 (Accession number AAF99922).

Morpholinos

Morpholinos were obtained from Gene Tools, LLC (Corvallis, OR, USA). All morpholinos were arbitrarily designed to bind to sequences flanking and including the initiating methionine. We selected sequences based on design parameters according to the manufacturer's recommendations (21-25mer antisense), and tested each design sequence for representation elsewhere in the genome (Nasevicius and Ekker, 2000). Sequences were as follows (the sequence complimentary to the predicted start codon is shown in bold in all cases): PSR-MO, 5′-TCCgTTTCTTgCTTTTATggTT**CAT**-3′; and control-MO, 5′-TCCCTTACTTgCATTTATCgTACAT-3′. The five sites in the control sequence that are subject to point mutation in the PSR-MO sequence are underlined.

Injection of *psr* morpholinos

Morpholino oligonucleotides were solubilized in water at a concentration of 1mM, and diluted with water to 0.5, 0.25 and 0.125 mM prior to injection (1.5-3 nl) into the yolk (Ekker et al., 1995).

In situ hybridization

Digoxigenin-labeled antisense RNA probes were synthesized from linearized DNA templates, including *psr*, *pax2.1* and *nkx2.5*, using T7 RNA polymerase (Boehringer Mannheim, Germany). Whole-mount in situ hybridization was performed as previously described (Xu et al., 1994). The in situ hybridization assay used embryos injected with PSR-MO or control-MO at 12 hpf, 36 hpf or 3 days post-fertilization (dpf).

Apoptotic cell staining

Embryos at the one- or two-cell stage were injected with PSR-MO or control-MO. They were harvested at 12 and 24 hpf, and fixed with 4% paraformaldehyde in PBS (pH 7.4) at room temperature for 30 minutes. The embryos were stained with Acridine Orange (1 μg ml^{-1}) for 3-5 minutes, washed twice in PBS, and evaluated under fluorescence microscopy (using incident light at 488 nm excitation, with a 515 nm longpass filter for detection) (Hong et al., 1998). For the TdT-dUTP labeling step, the embryos were fixed in paraformaldehyde at the end of the incubation period (12 and 24 hpf), dechorionated, and incubated in blocking solution (0.1% H_2O_2 in methanol) for 30 minutes at room temperature. Embryos were rinsed with PBS, incubated on ice in a solution of 0.1% Triton X-100 in 0.1% sodium citrate for 30 minutes, to increase permeability, and rinsed twice with PBS. Afterwards, 50 μl of TUNEL reaction mixture (in-situ cell death-detection Kit, Boehringer Mannheim, Germany) was added and the embryos were incubated in a humidified chamber for 1 hour at 37°C. Embryos were analyzed for positive apoptotic cells under a fluorescence microscope equipped with a spot II cool CCD (Diagnostic Instruments, Sterling Heights, MI, USA).

Western blotting

Embryos were injected with PSR-MO or control-MO at the one- or two-cell stage. They were harvested at 24 hpf and lyzed in 150-200 μl sodium dodecyl sulfate (SDS) sample buffer [0.63 ml 1 M Tris-HCl (pH 6.8), 1.0 ml glycerol, 0.5 ml β-mercaptoethanol, 1.75 ml 20% SDS, 6.12 ml H_2O in a total of 10 ml]. Protein from 40 μg of 24 hpf embryos was loaded on to each lane. Standard western-blot analysis was conducted using a human anti-PSR monoclonal antibody (Cascade Bioscience, Winchester, MA, USA) and a mouse anti-actin monoclonal antibody (Chemicon, Temecula, CA, USA). PSR was visualized using horseradish peroxidase-conjugated anti-mouse immunoglobulin (IgG) and the ECL

detection kit (Amersham Pharmacia Biotech, Denmark) (Hong et al., 1999).

Microinjection of *psr* mRNA

Zebrafish *psr* was cloned into the pCDNA3 vector, which contains a T7 RNA polymerase promoter site. Linearized plasmid DNA was used a template for in vitro transcription with the Message Machine Kit (Ambion, Austin, TX, USA), according to the manufacturer's instructions. For rescue of defective morphants, 0.1 nl of 200 ng/μl mRNA encoding soluble *psr* mRNA and PSR-MO (0.5 μM) were injected into the one-cell stage of each embryo using a gas-driven microinjector (Medical System Corporation) (Ekker, 1995).

Results

Time course of apoptotic cell death

Apoptotic death occurred during shield stage (Fig. 1A). Approximately four percent of embryonic zebrafish cells showed apoptotic death (Fig. 1B). Apoptotic cells possessed a multitude of membrane-enclosed micronuclei. Fig. 1C shows an apoptotic body displaying these micronuclei, as well as a normal-looking nucleus, being engulfed by a neighboring cell. The dying cells migrated to the margin of the yolk sack, either at the shield stage or at the two-to-three segmentation stage.

psr cloning and determination of functional domains

psr was cloned using a zebrafish-specific 500 bp probe to screen the 24 hpf cDNA library. The three positive clones that were obtained were used to search GenBank databases. Some significant matches were made after translating the nucleotide sequences to amino acid residues (Fig. 2A).

When we compared the nucleotide sequence identity of zebrafish *psr* (*zfpsr*) (AF401485) with other species, the match was 76% for *D. melanogaster*, 74% for human (KIAA0585) and 72% for mice (AF304118). The corresponding figure for *C. elegans*, from the hypothetical protein F29B9.4 (U70848), was 60%.

The predicted molecular weight (Fig. 2A) for F29B9.4 was 44.3 kDa, based on sequence analysis (Fig. 2A). This is similar to the corresponding molecular weight for the mouse species (Fadok et al., 2000), slightly smaller than the corresponding figure for the gene products in humans (45.5 kDa) and *D. melanogaster* (45 kDa), but larger than the analogous figure for *C. elegans* (38.4 kDa). In addition, the consensus sequence for the PSR-binding motif (FxFxLKxxxKxR) found in protein kinase C isoforms indicates that a 12-amino acid peptide motif is responsible for the specific interaction with PSR (Igarashi et al., 1995). A potential tyrosine phosphorylation site is indicated by box A (Fig. 2A), corresponding to residues 100-108 (KCGEDNDGY), which is well within the predicted intracellular domain (Schultz et al., 2000). We found that the sequence indicated by box B (residues 143-206) resembled the jmjC domain that is part of the cupin metalloenzyme superfamily that can regulate the chromatin-reorganization process (Clissold and Ponting, 2001). Presently, the function(s) of the PSR region is unknown.

The protein sequence of topology programs varied slightly in their specific assignments (see box C; FVPGGWWHVVLNLDTTIAITQNF, residues 257-287 of PSR-F), based on an assessment of topology and possible hydrophobicity (SMART-TMHMM2) (Schultz et al., 2000). The predicted extracellular domain (indicated by box D) of the membrane-associated domain (residues 340-359) contains a serine-rich sequence (342-355) that may be glycosylated sites.

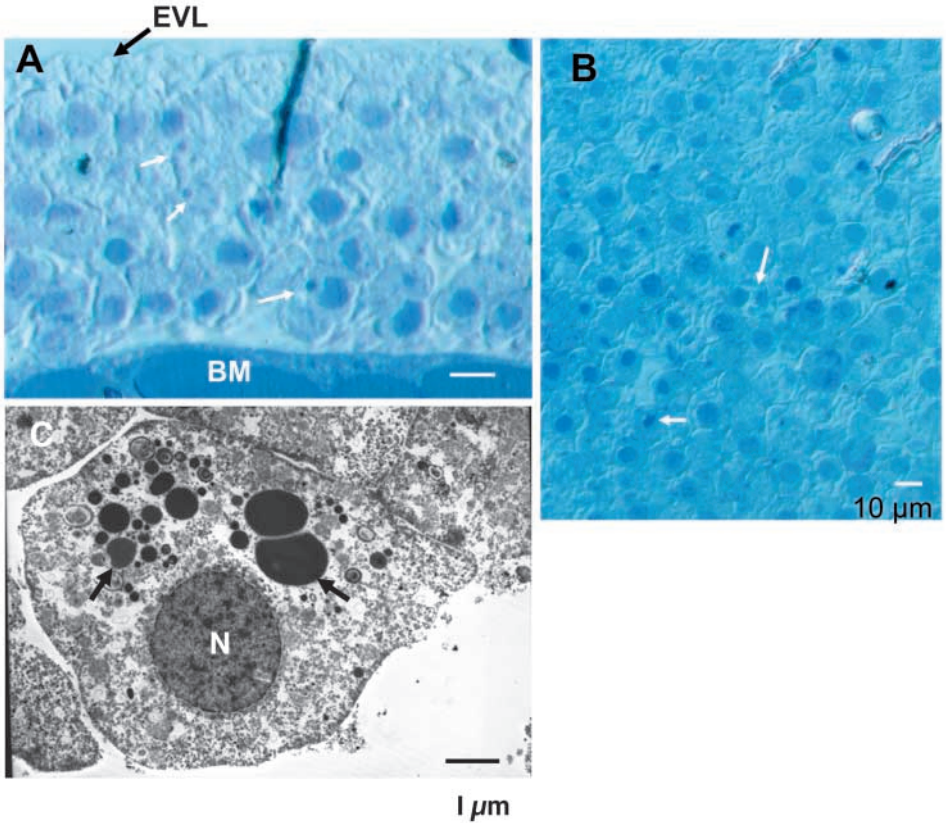

Fig. 1. Electron micrographs of apoptotic cell death within the zebrafish embryo at shield stage. (A) A vertical view of a zebrafish embryo at shield (6 hpf) stage, revealing an apparently normal developmental pattern that includes the enveloping layer (EVL; black arrow), an apoptotic cell (short arrow) and a phagocytotic cell (long arrow). These features are located at the deep cell multilayer, 4-5 cell layers from the blastoderm margin (BM). (B) A horizontal view of a zebrafish embryo at the shield (6hpf) stage. The apoptotic cell corpses include a highly condensed chromatin cell (short arrow). A substantial quantity of enclosed membrane material derived from multi-micronuclei (long arrow) suggests that the apoptotic cell is entering the late apoptotic cell stage. (C) An apoptotic cell engulfed by neighboring cells, revealing a normal nucleus (N) and a substantial quantity of multi-micronuclei (arrows). Scale bars: 10 μM in A,B; 1 μM in C.

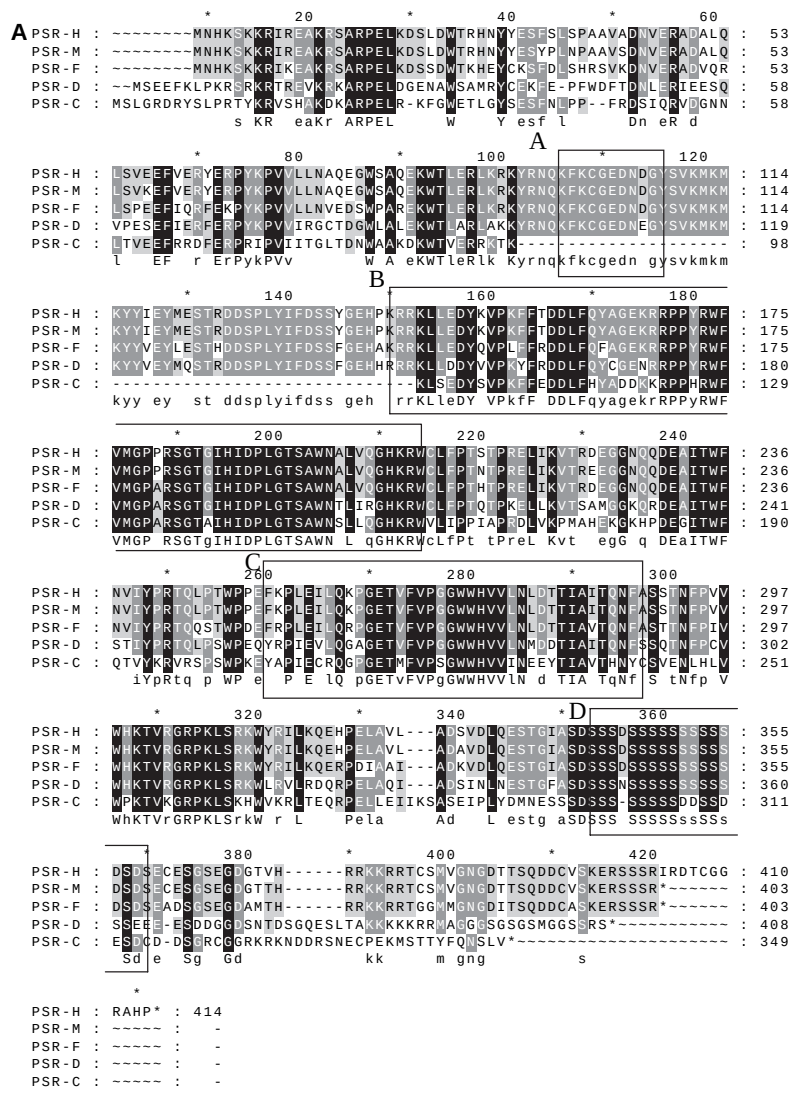

Fig. 2. Sequence alignment of zebrafish *psr* and its expression profile. (A) A sequence alignment of the PSR protein with the positions of the functional domains shown and indicated by a series of boxes labeled A-D. Box A reveals a potential tyrosine phosphorylation site (from 100-108 aa; KCGEDNDGY), which lies within the predicted intracellular domain (SMART-TMHMM2). The jmjC, A domain (residues 143-206) depicted in box B is part of the cupin metalloenzyme superfamily. In box C (residues 257-287) is an estimate of the secondary structure based upon an assessment of topology (SMART-TMHMM2) and possible hydrophobicity domains. The membrane-associated domain (340-359) contained within box D predicts (SMART-TMHMM2) an extracellular domain that contains the rich supply of serine that potentially may be glycosylated site in this domain. In the block are included all species that are show the complete identity sequences and with the partial identity sequences in all species being shadowed. PSR-H: human PSR; PSR-M: mouse PSR; PSR-F: zebrafish PSR; PSR-D: *Drosophila* PSR; PSR-C: *C. elegans* PSR. (B) Expression pattern of PSR from early to late developmental stages probed by in situ antisense RNA hybridization. PSR staining was visualized with a blue color. Topic view of embryos shown in panels a-b, lateral view shown in panels d-f, anterior is to the right side. (a) 512-cell stage, *psr* is expressed in all cells examined. (b) 30% epiboly, *psr* is expressed only near the margin of yolk syncytial layer. (c) 2-3 somites, *psr* are expressed in the whole embryo including the ectoderm, mesoderm and endoderm especially, with the major location for psr being within the brain region (indicated by arrow) and the posterior of the embryo. (d) 24 hpf, *psr* is expressed principally in the whole notochord (indicated by arrow) from the anterior to the posterior regions, and secondarily distributed in the trunk, brain and the eyes. (e) 36 hpf, *psr* is expressed similarly to that for 24 hpf but here, *psr* can be seen to be expressed in the hatching gland and posterior of somite (indicated by arrow). (f) 3 dpf, the *psr* can be seen to be expressed in some organs such as the heart and the kidney (indicated by arrow). Scale bars denote 100 μm.

psr expression pattern

psr was expressed in embryos from the one-cell developmental stage (30 minutes; data not shown) to the 3 dpf larval stage (Fig. 2B, panels a-f). After the somite segmentation period, *psr* was apparent throughout the embryo (Fig. 2B, panels c-e) and the hatching grand (Fig. 2B, panel e). At the larval (3 dpf) stage, *psr* expression was detected in the heart and kidney (Fig. 2B, panel f).

Effects of *psr* knockdown

PSR morpholino oligonucleotides (MO; 40 ng) were injected into embryos to accomplish knockdown of *psr* expression (Fig. 3). *psr* knockdown at the epiboly stage strongly affected embryonic morphological formation at 12 hpf, and produced a severe delay in epiboly formation (Fig. 3F), when compared with control embryos (Fig. 3E). In addition, cell corpses accumulated between the somite boundaries, close to the notochord, at the

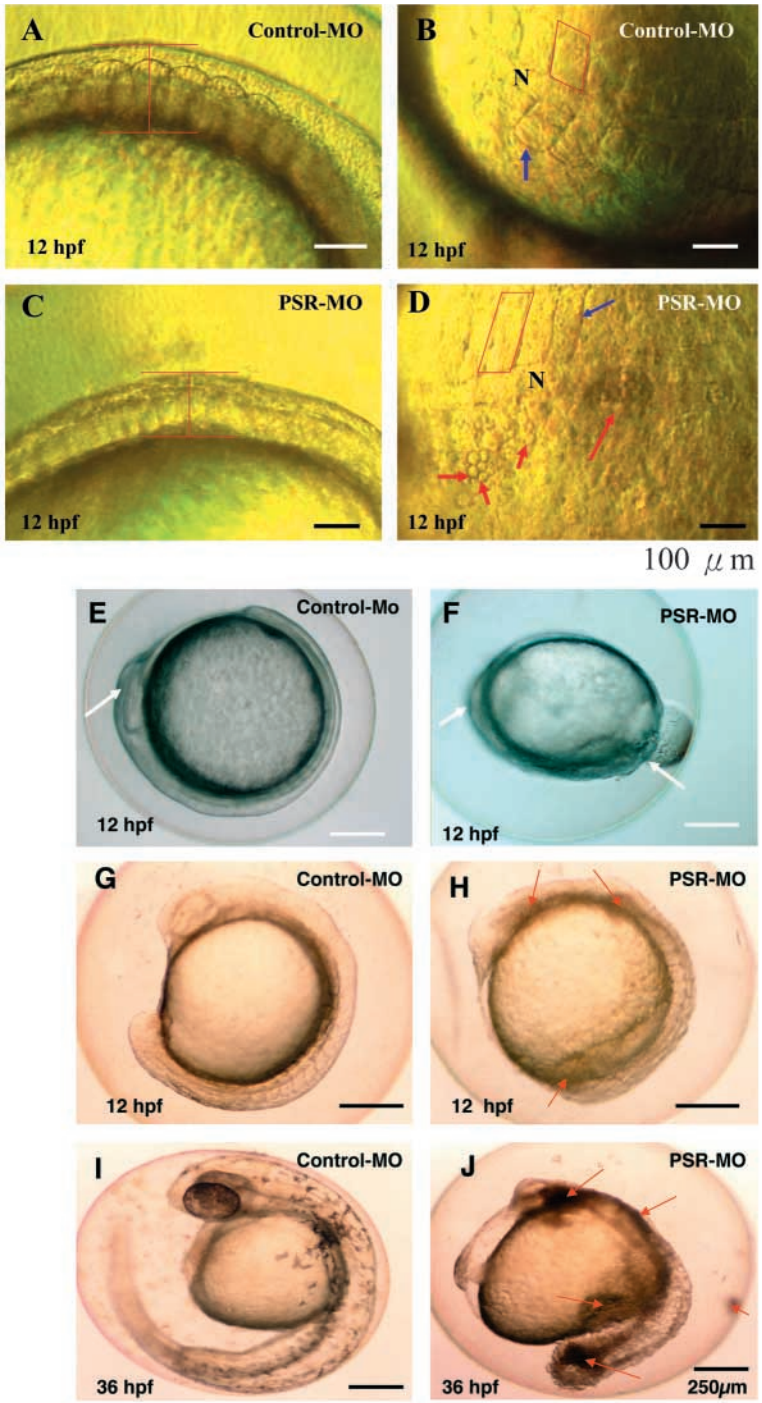

Fig. 3. Morpholino-induced knockdown of *psr* results in the loss of the cell corpse-engulfment process and cell migration. (A,B) Control-MO-injected embryos. Lateral (A) and top (B) views of the normal somite (open square and arrow) reveal the clear furrow of somite at the 6-somites stage (12 hpf). (C) Lateral view of a PSR-MO-injected embryo reveals abnormal development of the somite. There is no evidence of the clear furrow and the somite is thinner. (D) In PSR-MO embryos, a substantial number of cell corpses accumulate in the somite region (arrows), and an apparent 'hole' (long arrow) is formed on the surface of the somite. Scale bars: 100 μM. (E) In the control-MO group, complete epiboly and a normal brain (arrow) are observed; the clear bar of the eye can be seen. (F) In the PSR-MO group, incomplete epiboly (long arrow) and an abnormal brain (short arrow) are seen; the eye bar is not clearly evident. Scale bars: 250 μM. (G-J) The sequential pattern of cell corpse accumulation in whole embryos from 12-36 hpf. Embryonic cells were injected with control-MO and PSR-MO (40 ng per embryo) at the one-cell stage to block translation of the *psr* mRNA. (G,I) Control-MO groups at 12 hpf (G) and 36 hpf (I); embryos appear normal and no accumulation of cell corpses is evident. (H,J) PSR-MO groups at 12 hpf (H) and 36 hpf (J); embryos are abnormal and a gradual accumulation of corpse cells can be seen (arrows). Scale bars: 250 μM.

six-to-seven segmentation stage (Fig. 3D). Embryos treated with control-MO did not display cell corpses in the somite or near the notochord (Fig. 3B). PSR-MO embryos appeared to be thin from an anterior lateral view, with the loss of furrow from within the somite (Fig. 3C), when compared with control embryos (Fig. 3A).

Observation of embryonic development at different stages revealed that the initial accumulation of the corpse cells in the brain, interior somite and tail bar (Fig. 3G,H, 12 hpf) is followed by the gradual expansion of the zone of cell death (Fig. 3I,J, 36 hpf).

We next examined whether the cell corpses underwent apoptotic death (Fig. 4). Apoptotic corpses were covered in the furrow (indicated by arrows in Fig. 4), and lay close to the surface of individual somites at 14 hpf (Fig. 4C). After this time, a gradual increase in numbers and accumulation throughout embryos treated with *psr* oligonucleotides was evident (Fig. 4A,B, 17 hpf). Cell corpses leaked out from the 17 hpf embryos (Fig. 4B) that displayed chromatin condensation (Fig. 4D,E) in the corpse cells. Positive apoptoic cells were also evident in whole embryos at 17 hpf upon examination by the TUNEL assay (Fig. 4F-I).

Influence of cell corpses on normal embryonic development

We next tested the ability of the PSR-MO and the control-MO to block translation. As shown in Fig. 5A (panel a), injections of 10 and 40 ng of PSR-MO blocked between 70% (lane 4) and 90% (lane 5) of the normal protein expression. While the predicted molecular weight of the zebrafish PSR is 44.3 kDa, the protein evident in lane 4 migrated as two bands that were approximately 62 and 59.7 kDa species. This apparent discrepancy was likely due to the glycoprotein nature of PSR. Glycosylation could be subject to interference

Table 1. Percentage of morphant phenotypes during knockdown of *psr* by PSR-morpholinos

	PSRM5-MO	PSR-MO			
Phenotype	40 ng	5 ng	10 ng	20 ng	40 ng
Number of embryos	194	209	238	160	224
Normal	98%	92.5%	62.5%	21%	10%
Weakly defective	2%	7.5%	33%	56%	47%
Severely defective	–	–	2.5%	13%	28%
Death type	–	–	2%	10%	15%

All embryos were examined at 3 dpf.

following PSR-MO-mediated *psr* knockdown. At the 36 hpf stage, the PSR-MO (40 ng) samples showed a defective phenotype that reflected a loss of normal morphogenesis and a distorted *psr* expression pattern (Fig. 5B, panels b,c; as indicated by arrows), when compared with control-MO (Fig. 5B, panels a). Embryos at the 3-dpf stage displayed similar

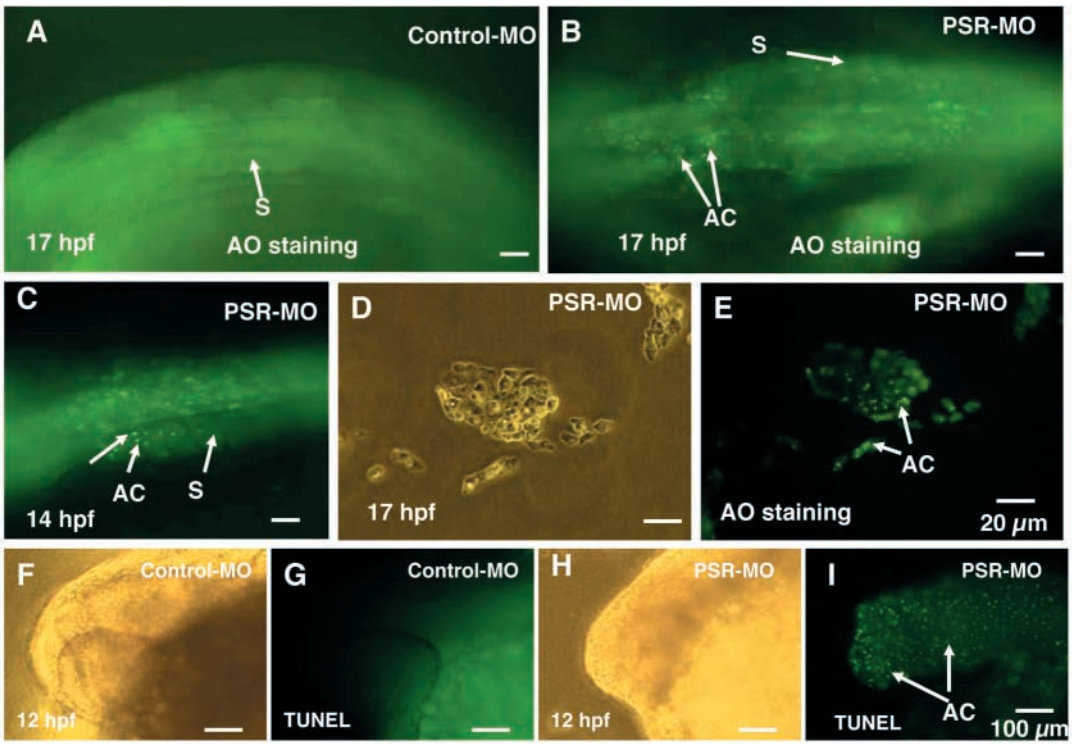

Fig. 4. Apoptotic cells identified by Acridine Orange staining and TUNEL assay. Embryonic cells were injected with control-MO or PSR-MO (40 ng per embryo) at the one-cell stage to block translation of *psr* mRNA. (A-C,E) Acridine Orange staining of 17 hpf control-MO (A), 17 hpf PSR-MO (B), 14 hpf PSR-MO (C) and 17 hpf PSR-MO (E) embryos. (D) Phase-contrast image of the PSR-MO group at 17 hpf. (F-I) TUNEL assay at 12 hpf stage. (F,H) Phase-contrast images of control-MO (F) and PSR-MO (H) groups. (G,I) Observation of the embryos under a fluorescent microscope allows the identification of positive apoptotic cells in the PSR-MO group (I), when compared with the control-MO group (G). (D,E) Corpse cells released (see B) accumulate predominantly in the furrow between somites. AC, apoptotic cells; S, clear somites. Scale bars: 100 μM.

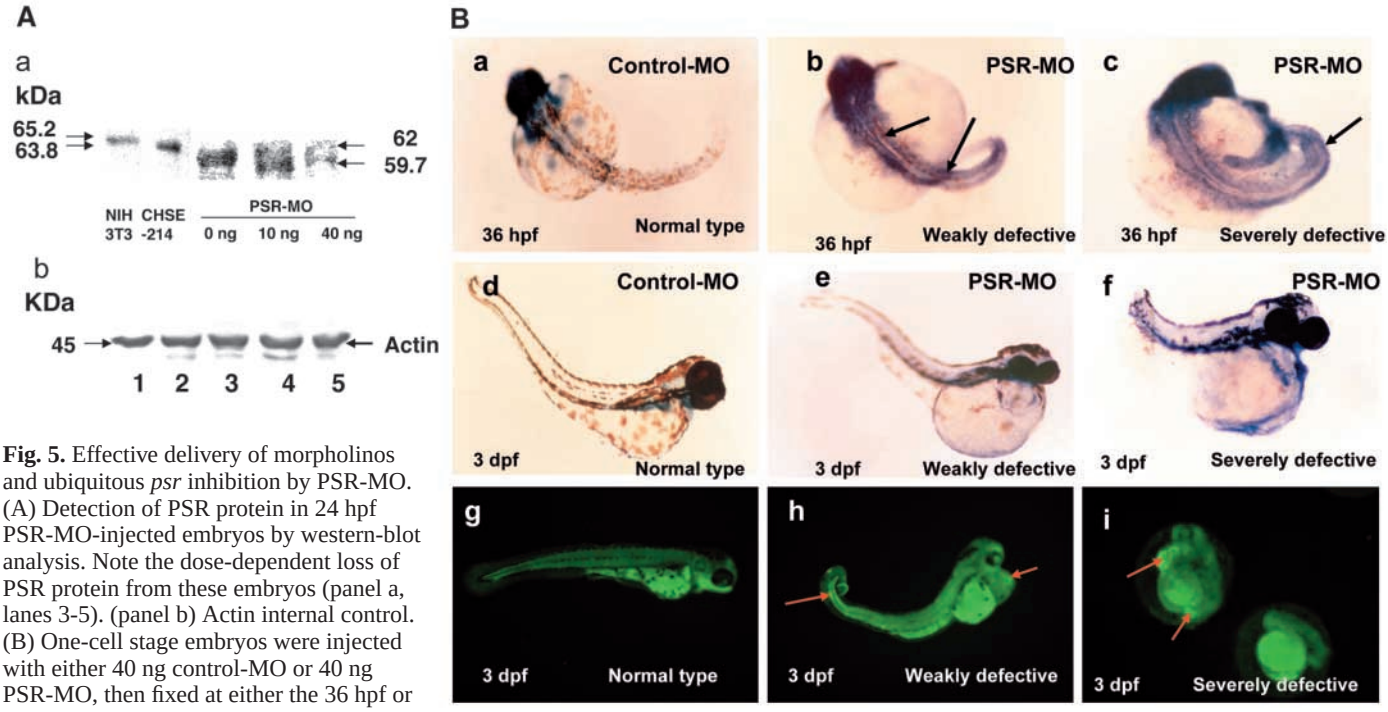

Fig. 5. Effective delivery of morpholinos and ubiquitous *psr* inhibition by PSR-MO. (A) Detection of PSR protein in 24 hpf PSR-MO-injected embryos by western-blot analysis. Note the dose-dependent loss of PSR protein from these embryos (panel a, lanes 3-5). (panel b) Actin internal control. (B) One-cell stage embryos were injected with either 40 ng control-MO or 40 ng PSR-MO, then fixed at either the 36 hpf or 3 dpf stage for in situ hybridization. (a,d) Phase-contrast images of the control-MO group, showing normal embryonic development and *psr* expression patterns. (b,c,e,f) Phase-contrast images of the PSR-MO group, showing abnormal development, with delayed (b,arrows) or distorted (c, arrows) *psr* expression patterns. (g-i) Fluorescence microscopy of an Acridine Orange-stained control-MO embryo (g), a weakly defective PSR-MO embryo (h) and a severely defective PSR-MO embryo (i). Accumulated corpse cells are indicated by arrows.

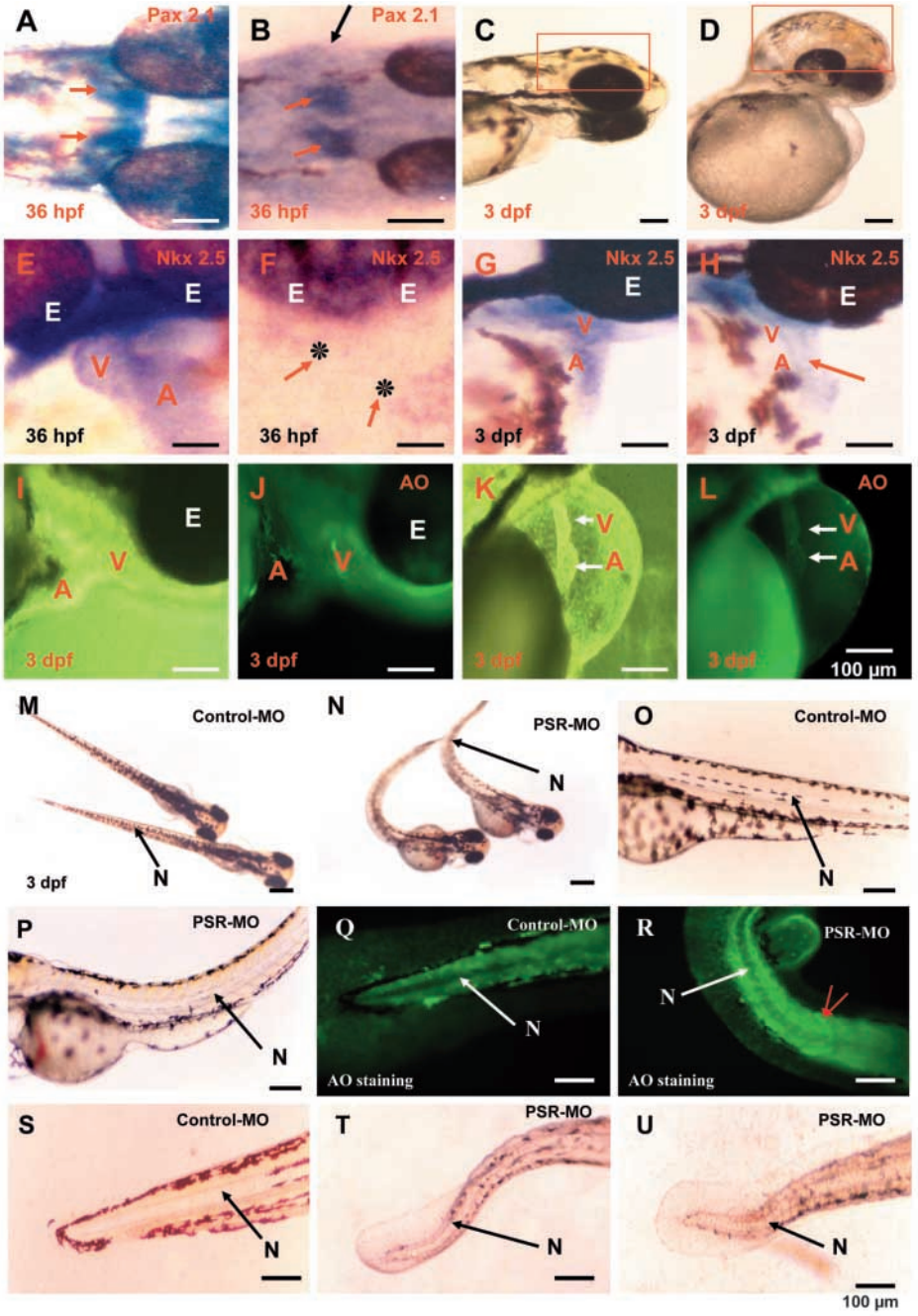

Fig. 6. Morpholino-induced knockdown of *psr* results in defective brain, heart and notochord development. Morphological analysis of embryos injected with 40 ng control (A,C,E,G,I,J) or PSR morpholinos (B,D,F,H,K,L), and examined at 36 hpf (A,B,E,F) or 3 dpf (C,D,G-I), following staining for *pax2.1* (A,B) or *nkx2.5* (E-H), or with Acridine Orange (AO; I-L), or in the absence of stain (C,D). (A,B) Top view, anterior to the right; stained with *pax2.1*. (C,D) Lateral views. The PSR-MO-injected embryo (B) shows an enlarged brain (long arrow) and an abnormal *pax2.1* expression pattern (short arrows), when compared with the control-MO-injected embryo (A). The enlarged brain includes fore-, mid- and hindbrain morphologies (indicated by the open square in Fig. 6D; comparative control is shown in C). (E-L) Investigation of heart development. (E-H) At 36 hpf, the PSR-MO-injected embryos reveal an absence of normal heart formation (F, arrows and asterisks), when compared to the atria (A) and ventricles (V) observed in controls (E). By 3 dpf a tube-like heart has formed in the PSR-MO-injected embryos (H,K,L; arrows), as compared with normal controls (G,I,J). (M-U) The effect of knockdown of *psr* on notochord formation at 3 dpf. PSR-MO-injected embryos (N,P,R,T,U) show abnormal morphological formation such as the bending of the notochord (N, arrows), when compared with the control-MO group (M,O,Q,S). Scale bars: 100 µM.

alterations (Fig. 5B, panels e,f; as indicated by arrows), as compared with control (Fig. 5B, panel d).

Acridine Orange staining of abnormal 3 dpf embryos revealed both weakly and severely defective phenotypes (Fig. 5B, panels h,i), compared with the control-MO group (Fig. 5B, panel g). In the relatively few embryos that displayed the weakly defective phenotype, bending of the notochord or a slight delay in heart development prior to hatching was evident (Fig. 5B, panels e,h). Conversely, the severely phenotypically defective embryos exhibited marked developmental impediments, such as shrinkage of the brain, loss of posterior somite development, and failure to hatch out (Fig. 5B, panels f,i).

We estimated the effect of different individual doses of PSR-MO (5 ng, n=209; 10 ng, n=238; 20 ng, n=160; 40 ng, n=224; control-MO, 40 ng, n=194) on embryonic development. As summarized in Table 1, developmental effects correlated to PSR-MO dosage, and were significant when compared with control-MO-injected embryos.

psr involvement in organogenesis

Brain and heart development were monitored by the use of the marker genes *pax2.1* (Klaus and Brand, 1998) and *nkx2.5* (Schwartz and Olson, 1999), at 12, 24, 36 and 72 hpf. Significant differences were apparent at 12 and 24 hpf (data not shown) between PSR-MO- and control-MO-injected embryos. The developing mid- and hindbrains of PSR-MO-injected embryos appeared shrunken and displayed an abnormal *pax2.1* expression pattern at 36 hpf (Fig. 6B), when compared with the control (Fig. 6A). At 3 dpf, there was about a 2-fold shortening of the mid- and hindbrain regions (indicated by the open squares in Fig. 6D), when compared with the control-MO group (Fig. 6c). Knockout of *psr* affects brain development in mice (Li et al., 2003).

Probing with *nkx2.5*, or staining with Acridine Orange, allowed the monitoring of heart development and its overall morphogenesis. Based on an in situ assay conducted at the 36 hpf stage, the heart suffered a severe developmental delay that was manifest as an absence of the atria and ventricles (Fig. 6E,F). At the 3 dpf stage, the formation of a tube-like heart and an abnormal blood-circulation rate was noted (Fig. 6G,H). Defective

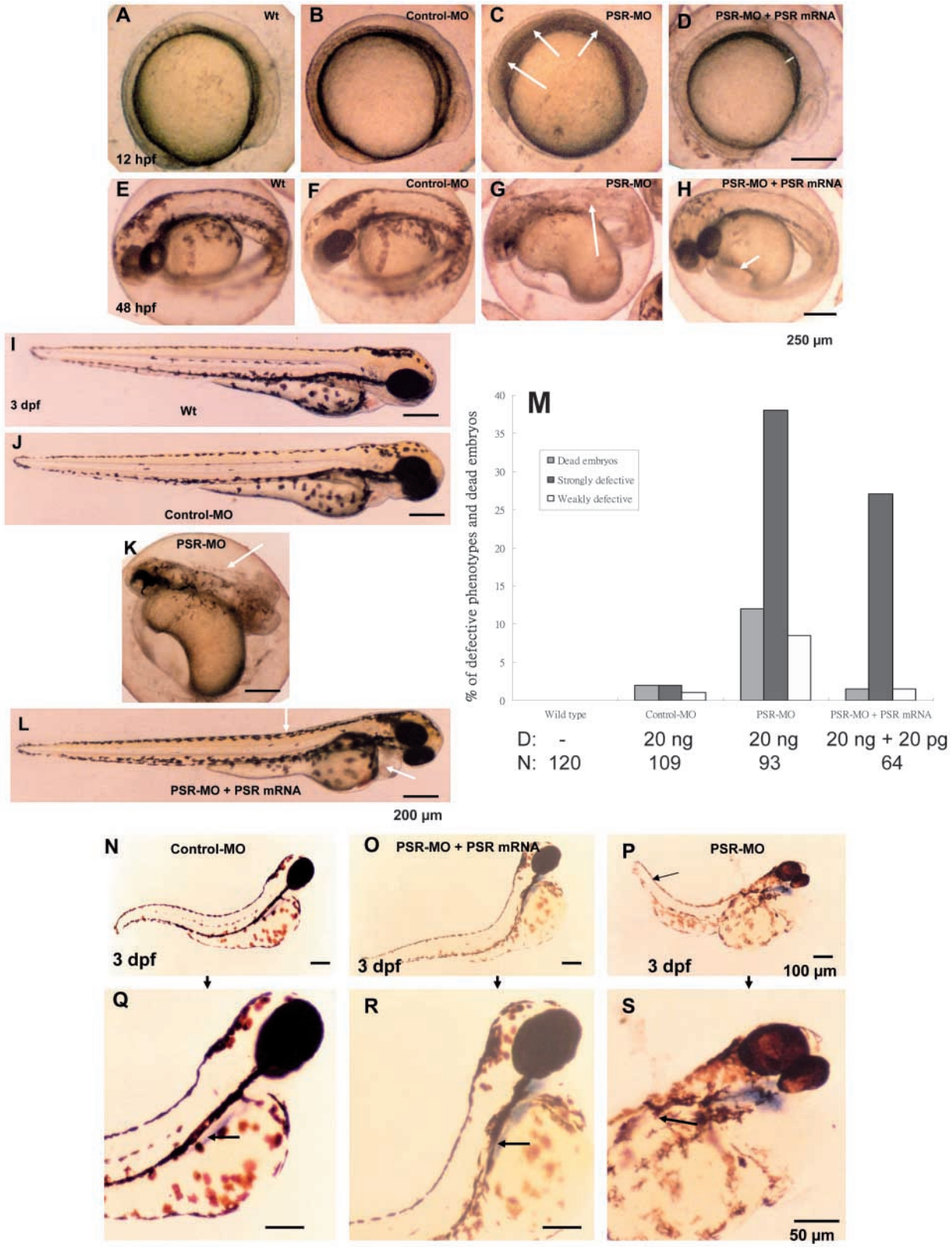

embryos had a heart cavity that was enlarged up to 60% more than normal size, and displayed abnormal heart formation (Fig. 6I-L). The different phenotypes of the notochord are shown in Fig. 6M-U. The top view of PSR-MO larvae revealed a substantial bending of the notochord (Fig. 6N), when compared with control-MO larvae (Fig. 6M). From a lateral view, the defective embryos showed bending of the notochord between the interior-posterior and posterior positions (Fig. 6N,P,R,T), when compared with the control-MO group (Fig. 6O,Q,S). Acridine Orange staining revealed a substantial number of

Fig. 7. The PSR morpholino-induced defect morphant can be rescued by injection of *psr* mRNA. PSR-MO at 20 ng and *psr* mRNA at 20 pg were injected at the one- to two-cell stage, embryonic development was traced at 12 (A-D), 48 (E-H) and 72 (I-L) hpf. (A,E,I) Untreated embryos; (B,F,J,N,O) embryos injected with control-MO; (C,J,K,P,S) PSR-MO-injected embryos; (D,H,I,R,S) embryos injected with PSR-MO and *psr* mRNA. (A-D) By 12 hpf, PSR-MO-injected embryos had accumulated corpse cells in whole embryo (E, arrows); these were not observed in the rescued embryos (D), or in controls (A,B). (E-H) At 48 hpf, PSR-MO morphants were severely defective (G, long arrow), whereas embryos in the rescued group were only weakly defective (H, short arrow). The morphology of the control-MO-injected embryos (F) is comparable to that of wild type (E). (I-L) At 3 dpf, rescued embryos (L) were compared with PSR-MO-injected embryos (K), wild-type variants (I), and control-MO-injected embryos (J). In contrast to the severely-defective morphant (K), the trunk and heart cavity of rescued embryos (L, arrows) resembles those of wild-type (I) and control-MO (J) embryos. (M) Estimation of the protection ability of differing doses of *psr* mRNA. D, dose; N, number of embryos. (N-S) At 3 dpf, rescued embryos (O,R) reveal normal morphology and a normal *psr* expression pattern in the kidney (arrows), as shown in control-MO embryos (N,Q), when compared to the PSR-MO-injected embryos (P,S). Scale bars: A-H, 250 μM; I-L, 200 μM; N-P, 100 μM; Q-S, 50 μM.

apoptotic cells located in the posterior of the somite (Fig. 6R), when compared with controls (Fig. 6Q).

Rescue of defective morphants with *psr* mRNA

In a previous study (Bauer et al., 2001), 10-20 pg of *psr* mRNA compensated for the developmental blockage imposed by PSR-MO when co-injected with 20 ng of PSR-MO at the embryonic one- or two-cell stage. We observed that a similar application of 20 ng of PSR-MO and 20 pg of *psr* mRNA reproduced the earlier findings. In the PSR-MO group, embryos had accumulated many corpse cells in the whole embryo by 12 hpf (Fig. 7C). Accumulation was particularly evident in the furrow between somites. Conversely, in rescued embryos only a few corpse cells were evident in the interior somite (Fig. 7D). Wild-type or control-MO embryos did not show accumulated corpse cells (Fig. 7A,B).

At 48 hpf, PSR-MO embryos still displayed both weakly and severely defective developmental phenotypes (Fig. 7G). However, in rescued embryos examined at 48 hpf, only the weakly defective phenotype was detectable (Fig. 7H). Compare with these the normal phenotype of the wild-type and control-MO embryos (Fig. 7E,F). The two defective developmental phenotypes were evident, even at 3 dpf (Fig. 5B, panels e,f,h,i; Fig. 7K), in PSR-MO embryos. By comparison, rescued 'normal-like' morphants (Fig. 7L) showed a slightly different phenotype at 3 dpf, namely a bending of the trunk and heart cavity, when compared with wild type (Fig. 7I) and the control-MO group (Fig. 7J).

We estimated the survival ratio and morphants phenotype ratio in the PSR-MO plus *psr* mRNA group (n=64), and in the PSR-MO group (n=93) at 2 dpf. Addition of *psr* mRNA reduced mortality from 12.5 to 1.5% (Fig. 7M). Addition of

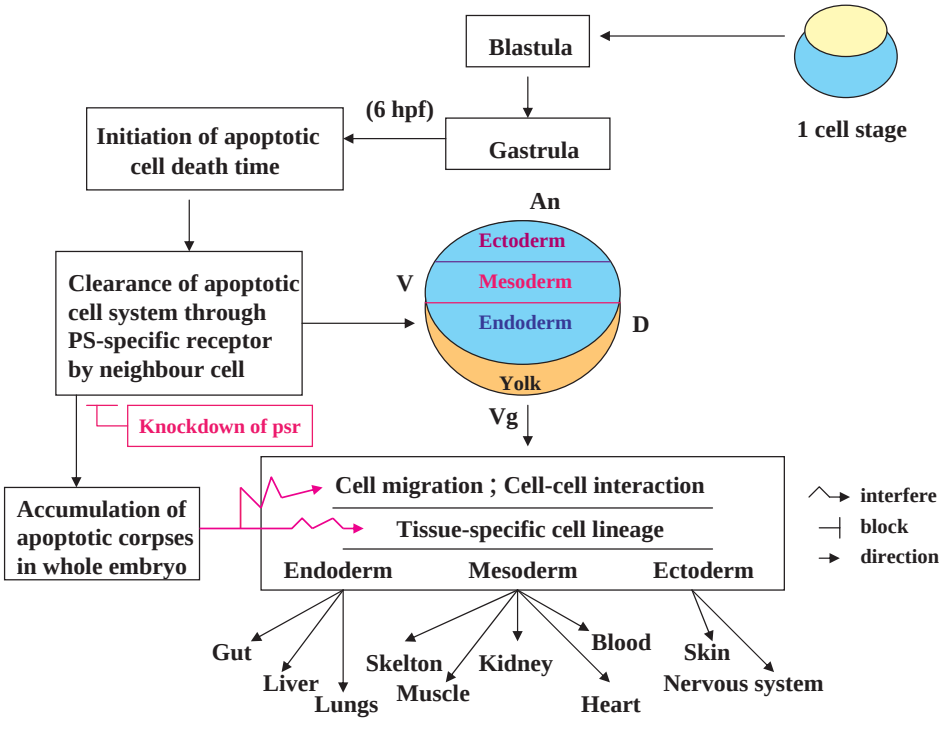

Fig. 8. Depiction of the hypothesis that PSR plays a crucial role in engulfing apoptotic cell corpses that affect normal embryonic development and organogenesis. The zygotic embryo is featured as a newly-fertilized entity through to the completion of the first zygotic cell cycle at zero hours, then at the cleavage stage (0.75 hpf), and cell cycles 2-7, which occur rapidly and synchronously. Embryos enter the blastrula at 2.25 hpf, at which time the metasynchronous cell cycles rapidly give way to a lengthening at the 8-10 cell-cycle stage, when the asynchronous cell cycles at the midblastula transition and epiboly commence. From 5.25 hpf, the gastrula begins development of the three germ layers, when all cells require the facility of cell movement in order to achieve their developmental goals, such as the morphogenetic movements of involution, convergence, and extension from the epiblast, hypoblast and embryonic axis through to the end of epiboly. During the early gastrula stage (6 hpf), apoptotic death can occur during the entrance to the shield stage, if the apoptotic cell corpses are not removed promptly. Inhibited removal can result from an absence of a specific engulfing receptor, such as the PSR. The accumulated corpses gradually and progressively impede the cell movement and cell-cell interaction necessary for the triggering of signaling to activate the downstream developmental events. At the onset of organ development, cells in the embryo are associated with one of three germ layers, the ectoderm, mesoderm and endoderm, from the time of segmentation (10 hpf), when somites, pharyngeal, primordia and neuromeres develop, for primary organogenesis, and for the proper appearance of the tailbud. This influences the morphogenesis of organs at the pharyngula (24 hpf), hatching (48 hpf) and early larval (72 hpf) stages.

psr mRNA reduced the morphants phenotype ratio from 38 to 28% for the strongly defective embryos, and from 9 to 1.5% for the weakly defective embryos (Fig. 7M). The rescued group showed a normal morphogenesis and kidney-development pattern (Fig. 7O,R), when compared to the control-MO group (Fig. 7N,Q) at the 3-dpf stage. At the same stage, the weakly defective embryos in the PSR-MO group displayed patterns of morphogenesis and *psr* expression that were indicative of delayed kidney development (Fig. 7P,S).

Discussion

Phagocytosis, the phenomenon caused by inflammation and autoimmune responses (Savill and Fadok, 2000; Wyllie et al., 1980; Henson et al., 2001), is an important process for modeling tissue during development (France et al., 1999). The link between phagocytosis and development thus provides a useful system with which to identify genes that are important for phagocytosis. These genes have been difficult to identify in more complex mammalian systems (France et al., 1999). Although some questions remain, PSR appears to play a central role in the clearance of apoptotic cells (Fadok et al., 2001).

Zebrafish as a model system for studying the engulfing gene from early to late development

The zebrafish (*Danio rerio*) has several advantages as a model for studying development (ZFIN website, http://zfish.uoregon.edu/) (Dooley and Zon, 2000). In our temporal study, we traced the path of abnormal development during the knockdown of *psr*. We detected three phenotypically different embryos (weakly defective, strongly defective and death type) during examinations at 12 and 36 hpf and 3 dpf. Although the weakly defective embryo was not apparent at 12 hpf, the defect was apparent at 3 dpf as a mild abnormality that included an enlarged heart cavity and defective notochord formation. The strongly defective embryo type at 12 hpf was characterized by the accumulation of a large number of apoptotic corpses in the posterior section of the embryo that interfered with the posterior development. This was also the case at 36 hpf, and the embryo failed to hatch out at 3 dpf. The death type embryo was characterized by an accumulation of a large number of cell corpses in the whole embryo at 12 hpf. The embryos were developmentally delayed at 36 hpf and died before the 3-dpf stage. Interestingly, the rescue studies that demonstrate that the death type, and the weakly and strongly defective phenotypes could be corrected or compensated for by the injection of *psr* mRNA (Fig. 7) suggest that *psr* mRNA could potentially be used to correct diseases arising from *psr* gene defects.

How apoptotic cell corpses interfere with cell migration and embryonic development

The present study offers support for our idea that the accumulation of cell corpses interferes with normal embryonic development by altering cell movement (Fig. 3E,F) and cell-cell interaction (Fig. 8).

The zebrafish embryo undergoes the first cell cycle at zero hours post-fertilization. Cell cycles 2-7 occur rapidly and synchronously. The embryo enters the blastula stage at 2.25 hpf, and the metasynchronous cell cycles become longer at the 8- to 10-cell cycle stage. Asynchronous cell cycles begin at the midblastula transition stage, when epiboly commences (Kimmel, 1995) (ZFIN website, http://zfish.uoregon.edu/). At the midblastula stage, the gastrula starts to emerge at 5.25 hpf and all cells acquire the ability to move. Movement is required by cells to achieve their developmental goals. These goals include the morphogenetic movement of involution, convergence and extension from the epiblast, hypoblast and embryonic axis through to the end of epiboly (Woo et al., 1995; Sampath et al., 1998; Heisenberg et al., 2000). If the apoptotic cell corpses are not quickly removed, they can impede cell movement. At the onset of organ development, cells are typically associated with one of three germ layers (ectoderm, mesoderm or endoderm) that participate in the development of somites, primordial pharyngea and neuromeres, and in primary organogenesis and tailbud formation (Kimmel et al., 1995; Woo et al., 1995). At this stage cell-cell interaction is also important (Mellitzer et al., 1999; Xu et al., 1999; Jiang et al., 2000). Finally, cell corpses gradually affect morphogenesis of normal organs at the pharyngula (24 hpf), hatching (48 hpf) and early laval (72 hpf) stages.

PSR is a professional clearer of cell corpses

PSR mediates the engulfment of apoptotic cells in mice (Fadok et al., 2000). A defect of PSR in the early stages of organogenesis may be involved in respiratory distress syndromes and congenital brain malformation (Li et al., 2003). In addition, studies in *C. elegans* (Wang et al., 2003) and *D. melanogaster* illustrate the power of using genetically tractable systems to identify essential phagocytic genes (Chung et al., 2000; Fares and Greenwald, 2001; Conradt, 2002). It is important to recognize that phagocytosis is performed by cells that are classified as 'non-professional' phagocytes, rather than by specialized phagocytes, such as macrophages in *D. melanogaster*. Here, we shed more light upon the role of this emerging phagocytosis receptor (PSR) in the vertebrate system (Savill and Fadok, 2000; Henson et al., 2001; Schlegel and Williamson, 2001; Li et al., 2003). Our results indicate that phagocytosis during the development of zebrafish is performed by PSR-mediated phagocytes, which are distributed throughout the entire embryo, especially between the 2- and 3-somite stage and 24 hpf, and that these are 'professional' phagocytes rather than non-specialized phagocytes.

We thank Mr H.-Y. Gong for the *pax2.1* plasmid and Dr J.-N. Chen for the *nkx2.5* plasmid. This work was partially supported by grants from the National Science Council, Taiwan, Republic of China awarded to J.-L.W. (NSC-90-2311-B-001-018) and J.-R.H. (NSC-91-2311-B-006-007; NSC-92-2313-B-006-005).

References

Arur, S., Uche, U. E., Rezaui, M. F., Scranton, V., Cowan, A. E., Mohler, W. and Han, D. K. (2003). Annexin I is an endogenous ligand that mediates apoptotic cell engulfment. *Dev. Cell* **4**, 587-598.

Bauer, H., Lele, Z., Rauch, G.-J., Geisler, R. and Hammerschmidt, M. (2001). The type I serine/threonine kinase receptor Alk8/Lost-a-fin is required for Bmp2b/7 signal transduction during dorsoventral patterning of the zebrafish embryo. *Development* **128**, 849-858.

Chung, S., Gumienny, T. L., Haengartner, M. O. and Driscoll, M. (2000). A common set of engulfment genes medistes removal of both apoptotic and necrotic cell corpses in *C. elegans*. *Nat. Cell Biol.* **2**, 931-937.

Clissold, P. M. and Ponting, C. (2001). jmjC: cupin metalloenzyme-like domains jumonji, hairless and phospholipaseA_2. *Trends Biochem. Sci.* **26**, 7-9.

Conradt, B. (2002). With a little help from your friends: cells don't die alone. *Nat. Cell Biol.* **4**, E139-E1394.
Dooley, Z. and Zon, L. I. (2000). Zebrafish: a model system for the study of human disease. *Curr. Opin. Genet. Dev.* **10**, 252-256.
Ekker, S. C., Ungar, A. R., Greenstein, P., von Kessler, D. P., Porter, J. A., Moon, R. T. and Seachy, P. A. (1995). Patterning activities of vertebrate hedgehog proteins in the developing eye and brain. *Curr. Biol.* **5**, 944-955.
Fadok, V. A., Bratton, D. L., Rose, D. M., Pearson, A., Ezkewitz, R. A. and Henson, P. M. (2000). A receptor for phosphatidylserine-specific clearance of apoptotic cells. *Nature* **405**, 85-90.
Fadok, V. A., Kue, D. and Henson, P. (2001). If phosphatidylserine is the death knell, a new phosphatidylserine-specific receptor is the bellringer. *Cell Death Differ.* **8**, 582-587.
Fares, H. and Greenwald, I. (2001). Regulation of endocytosis by CUP-5, the *Caenorhabditis elegans* mucolipin-1 homolog. *Nat. Genet.* **28**, 64-68.
Franc, N. C., Heitzler, P., Ezekowitz, A. B. and White, K. (1999a). Requirement for croquemort in phagocytosis of apoptotic cells in *Drosophila*. *Science* **284**, 1991-1994.
Franc, N. C., White, K. and Ezekowitz, A. B. (1999b). Phagocytosis and development: back to the future. *Curr. Opin. Immunol*. **11**, 7-52.
Heasman, J. (2002). Morpholino oligos: making sense of antisense? *Dev. Biol.* **243**, 209-214.
Heisenberg, C. P., Tada, M., Rauch, G. J., Saude, L., Concha, M. L., Geisler, R., Stemple, D. L., Smith, J. C. and Wilson, S. W. (2000). Silberblick/Wnt11 mediates convergent extension movements during zebrafish gastrulation. *Nature* **405**, 76-81.
Henson, P. M., Bratton, D. L. and Fadok, V. A. (2001). The phosphatidylserine receptor: a crucial molecular switch? *Nat. Rev. Mol. Cell Biol*. **2**, 627-633.
Hong, J. R., Lin, T. L., Hsu, Y. L. and Wu, J. L. (1998). Apoptosis procedes necrosis of fish cell line by infectious pancreatic necrosis virus. *Virology* **250**, 76-84.
Hong, J. R., Lin, T. L., Hsu, Y. L. and Wu, J. L. (1999). Dynamics of nontypical apoptotic morphological changes visualized by green fluorescent protein in living cells with infectious pancreatic necrosis virus infection. *J. Virol.* **73**, 5056-5063.
Igarashi, K., Kaneda, M., Yamaji, A., Saido, T. C., Kikkawa, U., Ono, Y., Inoue, K. and Umeda, M. (1995). A novel phosphatidylserine-binding peptide motif defined by an anti-idiotype monoclonal antibody. *J. Biol. Chem.* **270**, 29075-29078.
Jiang, Y. J., Aeme, B. L., Smithers, L., Haddon, C., Ish-Horowicz, D. and Lewis, J. (2000). Notch signalling and the synchronization of the somite segmentation clock. *Nature* **408**, 475-479.
Kimmel, C. B., Ballard, W. W., Kimmel, S. R., Ullmann, B. and Schilling, T. F. (1995). Stages of embryonic development of the zebrafish. *Dev. Dyn.* **203**, 253-310.
Klaus, L. and Brand, M. (1998). A series of *no isthmus (noi)* alleles of the zebrafish *pax2. 1* gene reveals multiple signaling events in development of the midbrain-hindbrain boundary. *Development* **125**, 3049-3062.
Lauber, K., Bohn, E., Krober, S. M., Xiao, Y. J., Blumenthal, S. G., Lindemann, R. K., Marini, P., Wiedig, C., Zobywalski, A., Baksh, S. et al. (2003). Apoptotic cells induce migration of phagocytes via caspase-3-mediated release of a lipid attraction signal. *Cell* **113**, 717-730.
Li, M. O., Sarkisian, M. R., Mehal, W. Z., Rakic, P. and Flavell, R. A. (2003). Phosphatidylserine receptor is required for clearance of apoptotic cells. *Science* **302**, 1560-1563.
Meier, P., Finch, A. and Evan, G. (2000). Apoptosis in development. *Nature* **407**, 796-801.
Mellitzer, G., Xu, Q. and Wilkinson, D. G. (1999). Eph receptors ephrins restrict cell intermingling and communication. *Nature* **400**, 77-81.
Nasevicius, A. and Ekker, S. C. (2000). Effective targeted gene knockdown in zebrafish. *Nat. Genet.* **26**, 216-220.
Platt, N., da Silva, R. P. and Gordon, S. (1998). Recognizing death: the phagocytosis of apoptotic cells. *Trends Cell Biol.* **8**, 365-372.
Ravichandra, K. S. (2003). Recruitment signals from apoptotic cells: invitation to a quiet meal. *Cell* **113**, 817-820.
Sampath, K., Rubinstein, A. L., Cheng, A. M., Liang, J. O., Fekany, K., Solnica-Krezel, L., Korzh, V., Halrem, M. E. and Wright, C. V. (1998). Induction of the zebrafish ventral brain and floorplate requires cyclops/nodal signalling. *Nature* **395**, 185-189.
Savill, J. (1998). Apoptosis: phagocytic docking without shocking. *Nature* **392**, 442-443.
Savill, J. and Fadok, V. (2000). Corpse clearance of defines the meaning of cell death. *Nature* **407**, 784-788.
Schlegel, R. A. and Williamson, P. (2001). Phosphatidylserine, a death knell. *Cell Death Differ.* **8**, 551-563.
Schwartz, R. J. and Olson, E. N. (1999). Building the heart piece by piece: modularity of *cis*-elements regulating *Nkx2.5* transcription. *Development* **126**, 4187-4192.
Schultz, J., Copley, R. R., Doerks, T., Ponting, C. D. and Bork, P. (2000). SMART: a web-based tool for the study of genetically mobile domain. *Nucleic Acids Res.* **28**, 231-234.
Summerton, J. and Weller, D. (1997). Morpholino antisense oligomers; design, preparation, and properties. *Antisense Nucleic Drug Dev.* **7**, 187-195.
Wang, X., Wu, Y. C., Fadok, V. A., Lee, M. C., Keiko, G. A., Cheng, L. C., Ledwich, D., Hsu, P. K., Chen, J. Y., Chou, B. K. et al. (2003). Cell corpse engulfment mediated by *C. elegans* phosphatidylserine receptor through CED-5 and CED-12. *Science* **302**, 1563-1566.
Westerfield, M. (ed.) (1993). *The Zebrafish Book*. Eugene, OR: University of Oregen Press.
Woo, K., Shih, J. and Fraser, S. (1995). Fate maps of the zebrafish embryo. *Curr. Opin. Gene Dev.* **5**, 439-443.
Wyllie, A. H., Kerr, J. F. and Currie, A. R. (1980). Cell death: the significance of apoptosis. *Int. Rev. Cytol.* **68**, 251-306.
Xu, Q., Holder, N., Patient, R. and Wilson, S. W. (1994). Spatially regulated expression of three receptor tyrosine kinase genes during gastrulation in the zebrafish. *Development* **125**, 3389-3397.
Xu, Q., Mellitzer, G., Robinson, V. and Wilkinson, D. G. (1999). *In vivo* cell sorting in complementary segmental domains mediated by Eph receptors and ephrins. *Nature* **399**, 267-271.